HHS Public Access

Author manuscript

Biomaterials. Author manuscript; available in PMC 2017 February 01.

Published in final edited form as:

Biomaterials. 2016 February ; 79: 79–87. doi:10.1016/j.biomaterials.2015.11.064.

Spatiotemporally Photoradiation-Controlled Intratumoral Depot for Combination of Brachytherapy and Photodynamic Therapy for Solid Tumor

Ratul Mukerji[a], **Jeffrey Schaal**[a], **Xinghai Li**[a], **Jayanta Bhattacharyya**[a], **Daisuke Asai**[b], **Michael R. Zalutsky**[c], **Ashutosh Chilkoti**[a], and **Wenge Liu**[a,*]

[a]Department of Biomedical Engineering, Duke University, Durham, NC 27708, USA

[b]Department of Microbiology, St. Marianna University School of Medicine, Kawasaki, Kanagawa Prefecture, Japan

[c]Department of Radiology, Duke University, Durham NC, 27708, USA

Abstract

In an attempt to spatiotemporally control both tumor retention and the coverage of anticancer agents, we developed a photoradiation-controlled intratumoral depot (PRCITD) driven by convention enhanced delivery (CED). This intratumoral depot consists of recombinant elastin-like polypeptide (ELP) containing periodic cysteine residues and is conjugated with a photosensitizer, chlorin-e6 (Ce6) at the N-terminus of the ELP. We hypothesized that this cysteine-containing ELP (cELP) can be readily crosslinked through disulfide bonds upon exposure to oxidative agents, specifically the singlet oxygen produced during photodynamic stimulation. Upon intratumoral injection, CED drives the distribution of the soluble polypeptide freely throughout the tumor interstitium. Formation and retention of the depot was monitored using fluorescence molecular tomography imaging. When imaging shows that the polypeptide has distributed throughout the entire tumor, 660-nm light is applied externally at the tumor site. This photo-radiation wavelength excites Ce6 and generates reactive oxygen species (ROS) in the presence of oxygen. The ROS induce *in situ* disulfide crosslinking of the cysteine thiols, stabilizing the ELP biopolymer into a stable therapeutic depot. Our results demonstrate that this ELP design effectively forms a hydrogel both *in vitro* and *in vivo*. These depots exhibit high stability in subcutaneous tumor xenografts in nude mice and significantly improved intratumoral retention compared to controls without crosslinking, as seen by fluorescent imaging and iodine-125 radiotracer studies. The photodynamic therapy provided by the PRCITD was found to cause significant tumor inhibition in a Ce6 dose dependent manner. Additionally, the combination of PDT and intratumoral radionuclide therapy co-delivered by PRCITD provided a greater antitumor effect than either monotherapy alone. These results suggest that the PRCITD could provide a stable platform for delivering synergistic, anti-cancer drug depots.

*Corresponding author at: Department of Biomedical Engineering, Duke University, Pratt School of Engineering: Room 136 Hudson Hall, Campus Box 90281, Durham NC 27708-0281, Tel: +1 919 660 5378, wengeliu@duke.edu (W. Liu).

Keywords

Elastin-like polypeptide; crosslinking; tumor retention; convection enhanced delivery; intratumoral drug delivery; photodynamic therapy

1. Introduction

The intratumoral (i.t.) administration of titanium encapsulated radionuclides, brachytherapy (BT), offers several desirable features: the predictable dosimetry of the titanium 'seeds', the capability of clinical monitoring, mild side effects, and short duration. Compared to external beam radiotherapy (EBRT), BT possesses key advantages: 1) BT irradiates tumor cells in an inside-out manner and avoids pass-through injury, unlike EBRT; 2) BT enables the use of higher doses (up to145 Gy) due to reduced side effects, while EBRT is limited to 70Gy [1]; 3) BT is more efficient than EBRT due to the "cross-fire" effect [2], and 4) conjugation with carrier does not alter the therapeutic activity of radionuclides as opposed to chemotherapeutic controlled release methods. Despite these advantages, certain constraints currently limit its applications in the clinic. These include the complicated placement procedures required for seed insertion, post-treatment excision of the seed implants, and occasional brachytherapy seed migration [3]. To improve upon these issues, polymeric nanoparticles carrying therapeutic radionuclides have recently been developed and demonstrated some success for use in brachytherapy [4–7]. Before these materials can be translated to clinical application, though, several delivery concerns must overcome. First, the macromolecular carrier carrying the radionuclide has to overcome the high interstitial fluid pressure of the tumor to penetrate into the interstitium [8]. Second, the delivered agents must be retained selectively at the target site for a sufficient time to allow the agents to kill the tumor cells. While challenging for chemotherapeutics, prolonged tumor retention of radionuclide over its decay half-life is even more imperative.

Convection-enhanced delivery (CED) is of great interest with regards to the issue of proper payload delivery. It enables direct localization of high concentrations of therapeutics within the tumor to maximize interstitial tumor distribution [9, 10]. The pressure gradient of the injected agent drives the therapeutics through the interstitial spaces of the tumor by convective flow. This results in a higher and more uniform concentration of therapeutic agents over a larger area. However, both free drug and their carriers can still be rapidly cleared from the tumor. In a related CED study, free drug concentration dropped by 25% at the injection site two hours after delivery and was decreased 10-fold at points 3 mm away [11]. In a second study, only 40% of initial dose of liposomal ^{186}Re was retained in the tumor after 4 hours [12]. To address the issue of intratumoral retention, stimulus-responsive polymers have gained popularity as improved drug delivery vehicles. For example, Pluronic (an F-127RT-Gel) exhibited 49% retention of In-111 after 24 hours in a mouse tumor [13]. Pronounced dose-dependent tumor growth reduction was also achieved by single dose of ^{131}I-labeled polymer poly(N-isopropyl acrylamide) in a murine xenograft model, a thermally responsive polymer that achieved a 48 day retention of 60% [14]. These materials utilized strategies that balanced intratumoral payload retention with the solubility necessary

for injection. To build on these findings, we turned to another class of stimulus-responsive polymers: elastin-like polypeptides (ELPs).

ELPs are a class of recombinant peptide polymers that mimic the structural sequence of the naturally occurring protein tropoelastin and provide an extremely attractive material for localized drug delivery. ELPs are composed entirely of repeats of the pentapeptide sequence Val-Pro-Gly-Xaa-Gly (where Xaa can be any amino acid except Pro). Because their composition consists entirely of natural amino acids, ELPs are biocompatible, biodegradable, and non-toxic [15–17]. To date, two approaches have been taken to optimize ELP-based depots for intratumoral delivery. In the first approach, an ELP with a transition temperature ($_t$) of 21°C was designed in order to undergo its inverse phase transition at physiological temperature. This ELP transitioned from soluble state to a viscous, insoluble state upon intratumoral injection and exhibited between 75–90% *in vivo* retention over a week [18, 19]. The conjugation of a radionuclide such as ^{131}I provided a means to perform brachytherapy by injection of an ELP-radionuclide conjugate that undergoes its phase transition to form an insoluble coacervate within the tumor, which irradiates the tumor from the inside out. While this approach is attractive due to its simplicity, these ELP depots are not chemically crosslinked, which can ultimately limit their *in vivo* retention. In the second approach, an ELP was engineered to contain periodic cysteine residues at the Xaa position. Co-delivery of low concentrations of hydrogen peroxide (H_2O_2) with this cysteine containing ELP (cELP) induced rapid oxidative, intermolecular disulfide mediated crosslinking after subcutaneous injection [20]. Because this approach required premixing the H_2O_2 with the cELP, neither the timing nor the coverage of the crosslinked depot could be controlled. In an effort to develop a temporal method for controlling the disulfide mediated crosslinking of cELP, we turned our attention to photodynamic therapy (PDT).

Since we have previously designed and synthesized cysteine containing ELP (cELP) that can readily crosslinked *in vitro* when pre-mixed with H_2O_2 [20], we hypothesized that the cELP crosslinking reaction could be induce by an photodynamic mechanism that could produce oxidative conditions. Specifically, the generation of the strong oxidative agent, singlet oxygen ($^1O_2$), could potentially crosslink ELP *in situ* [21]. In PDT, the molecular photosensitizer (PS) is externally excited by light of a specific wavelength, which then reacts with cellular oxygen to generate singlet oxygen ($^1O_2$) and other ROS [22]. These ROS can then oxidize the thiol moiety of cysteines to induce disulfide crosslinking. ROS can also induce tumor cell death through several indirect mechanisms, including damaging mitochondrial DNA in the cytoplasm (apoptosis), destabilizing the cell membrane (necrosis), or vascular shutdown [21]. PDT has been successfully against a spectrum of cancers and malignancies, including lung cancer, metastatic breast cancer, refractory ovarian cancer, malignancies of the esophagus and stomach [23–26]. For this study, Chlorine e6 (Ce6) was selected as the photosensitizer (PS), as it is activated by near infrared light at 660nm while generating singlet oxygen species in high yield. This is ideal for clinical application as the activation wavelength has relatively high penetration depth through tissue. The 660 nm LED was selected as the light source for the activation of Ce6 in this polymerization system.

In this study, we created a photoradiation controlled intratumoral depot (PRCITD) that enables spatial and temporal control of the delivery of intratumoral radionuclide therapy to provide optimized coverage and retention. The cELP was chemically conjugated with the Ce6 photosensitizer at the N-terminus. We hypothesized that the CED administration would drive the conjugate to uniformly diffuse throughout the tumor interstitium which could be monitored using fluorescence molecular tomography. Upon achieving optimal tumor coverage, application of 660-nm LED light would activate the Ce6 and crosslink the cELP into a stable hydrogel depot. Once formed, the hydrogel structure would enhance the exclusive retention of the cELP within the tumor for radionuclide therapy. Moreover, excess ROS generated through the photodynamic activation of the Ce6 would provide a combinatorial treatment modality to improve the overall tumor response (Figure 1). Once established, the PRCITD system is expected to be an attractive material for delivering combinatorial anti-cancer therapy that advances previous work in radionuclide brachytherapy [20] and could potentially be utilized in intratumoral chemotherapy strategies [27].

2. Materials and Methods

2.1. cELP Design and Gene Construction

The cysteine-containing ELP consists of 160 repeats of the pentapeptide sequence V-P-V-X-G, where X denotes an amino acid insert of either A, G or C in a ratio of 14:1:1, denoted ELP[A_{14}VC-16] or cELP. The cELP also had a C-terminal tyrosine tail (YGYGYGY) to facilitate conjugation to radioactive iodine. The recombinant ELP[A_{14}VC]$_{16}$ was synthesized as described previously [20] using the RDL method [28]. Briefly, the ELP [A_{14}VC]$_{16}$ gene was assembled by annealing sense and antisense oligonucleotide strands (Integrated DNA Technologies, Coralville, IA) to form a cassette. The gene was then subcloned into the EcoRI and HindIII sites of pUC19 (New England BioLabs, Beverly, MA) and oligomerized by RDL methods. The final oligomerized genes encoded for a 160 pentapeptide sequence, which was then excised from the pUC19 by digestion with PflMI and BglI. The gene was subcloned into the SfiI site of a modified pET-25b (+) vector (Novagen Inc, Madison, WI) and transformed into the expression host *E. coli* BL21(DE3) (EdgeBio, Gaithersburg, MD) for protein expression. The full cELP sequence is as follows: (S**K**GPG)-(VPVXG)$_{160}$-(YG)$_3$Y where the SKGPG leader sequence is used for enhanced expression in *E. coli*.

2.2. cELP Expression, Purification, and Characterization of Thermal Properties

cELP synthesis utilized constitutive expression of the leaky T7 promoter in the pET-25b plasmid in the *E. coli*. 50 mL of TB media (Mo Bio Laboratories, Carlsbad, CA) supplemented with 100 μg/mL ampicillin was inoculated from frozen cell stock and allowed to grow overnight at 37°C and 160 rpm. This culture was then evenly divided into 12 L of TB media with ampicillin and grown overnight at 37°C and 160 rpm. Cells were collected via centrifugation (4°C, 3000 rpm), suspended in phosphate buffered saline (PBS), and lysed by three rounds of ultra-sonication (Misonix, Farmingdale, NY). The lysate was treated with 1.2 wt% polyethyleneimine (PEI) and centrifuged (4°C, 14000 rpm) to precipitate out genomic DNA and other cellular debris. The supernatant, containing cELP, was then

purified by three rounds of inverse transition cycling (ITC), as described previously [28]. 20 mM tris(2-carboxyethyl)phosphine hydrochloride in PBS (pH 7) was used to resuspend the cELP in the first two rounds, to prevent unwanted disulfide bond formation, and dd-H_2O was used to resuspend the cELP in the final round of ITC. Yield was determined by lyophilization and measurement of dry cELP mass. Molecular weight and purity were verified using with SDS-PAGE protein gels stained with 0.5 M $CuCl_2$. ELP thermal properties were characterized by monitoring the change in optical density (OD) of an ELP solution as a function of temperature (1°C/min) at 350 nm on a temperature-controlled UV-Vis spectrophotometer (Cary 300 Bio; Varian instruments, Palo Alto, CA). The temperature at which the maximum of the first derivative of the turbidity profile occurs is defined as the T_t. The T_t of the cELP was measured in PBS over a range of concentrations from 0.5 – 3 mM. Prior to all animal experiments, endotoxins were removed from cELP samples incubation in Detoxi-Gel Endotoxin Removing columns (Thermo Scientific, Rockford, IL).

2.3. Conjugation of Ce6 Photosensitizer to cELP

Ce6 was selected as the photosensitizer as it generates $^1O_2$ in high yield and is activated by 660-nm light, which has a relatively high tissue penetration depth [29]. Ce6 was chemically conjugated to the N-terminus of cELP via a three-step reaction scheme [29]. First, 30 mg Ce6 powder (Frontier Scientific, Logan, UT) was reacted with 19 mg *N*-hydroxysuccinimide (NHS) and 34 mg dicyclohexylcarboiimide (DCC) in DMSO at room temperature under gentle stirring for 24 h. Second, 130 mg of cELP was dissolved in DMSO and added dropwise to the Ce6 reaction mixture on ice. 10 μL trimethylamine was added immediately afterward and the mixture was allowed to react at room temperature for 1–2 h. The resulting conjugate (Ce6-cELP) was dialyzed against PBS at 4°C for 1–2 h, and purified by gel filtration with a PD-10 column (GE Healthcare, Piscataway, NJ). cELP and Ce6 concentrations were determined by UV-Vis by measuring their absorbance at 280 nm and 400 nm respectively.

2.4. Radioiodination of cELPs

The cELPs were labeled with either ^{125}I or ^{131}I (PerkinElmer, Boston, MA) on the carboxyl-terminal tyrosine residues using the IODO-Gen method (GE Healthcare, Piscataway, NJ) [30]. Briefly, 100 μL of cELP were mixed with either 2 mCi Na[^{125}I] or 20 mCi Na[^{131}I] in an IODO-Gen pre-coated tube, reacted for 30 minutes, and then purified by gel filtration with a PD-10 column (GE Healthcare, Piscataway, NJ). The radioactivity was measure using a γ-counter (LKB-Wallac, Turku, Finland). The concentration of cELP was measured by UV-Vis spectrophotometry (Thermo Scientific, Waltham, MA) at a wavelength of 280 nm. The final concentration and radioactivity of iodinated ELP were adjusted by mixing with unlabeled ELP for an injection concentration (5 μCi/20μL of 0.25 mM ELP) and specific radioactivity (12 μCi/mg) for both *in vitro* stability and *in vivo* tumor retention studies; the injection concentration of [^{131}I]ELPs were 500 ~1500 μCi/20μL of 0.25 mM ELP with specific activity of 2–60 mCi/mg.

2.5. Conjugation of IRDye800 Fluorophore to cELPs

To monitor the trafficking and retention of cELP in the tumor, the N-terminal amine and the lysine residue (S**K**GPG)-$(VPVXG)_{160}$-$(YG)_3Y$ were conjugated with the IRDye800CW NHS ester. cELP (54 mg, 0.86 mmol) was dissolved in 1.2 mL of DMSO containing 8 μL of triethylamine. A solution of IRDye800CW NHS ester (LI-COR Biosciences, Lincoln, NE) containing 0.86 mmol in 0.3 mL of DMSO was prepared and added, and the reaction mixture was gently stirred for 1.5 h at room temperature. The IRDye800-cELP was purified by dialysis against water at 4°C for 1 h, followed by gel filtration with a PD-10 column. The labeling ratio was determined spectrophotometrically to be 0.11, using an extinction coefficient of 270,000 M^{-1} cm^{-1} at 780 nm for the IRDye800CW in a 1:1 mixture of PBS and methanol.

2.6. Optimization of cELP Crosslinking in vitro

Several combinations of cELP concentration, Ce6 concentration and LED exposure time were examined to find optimal crosslinking conditions. The cELP formulation for *in vitro* gelation tests was prepared by mixing Ce6 labeled cELP (Ce6-cELP) with unlabeled cELP to make the final Ce6 and cELP concentrations 5 – 150 μM and 0.5 – 2 mM respectively. A 660nm LED lamp (Mouser Electronics, Mansfield, TX) with a power of 170 mW/cm^2 served as the light source. Two *in vitro* experiments were designed to determine the variable dependency of gelation speed. First, the concentration of Ce6 in the mixture was varied from 5 – 150 μM while the cELP concentration was held constant at 0.5 mM. Next, the cELP concentration was varied from 0.5 – 2 mM while maintaining the Ce6 concentration at 150 μM. 100 μL of each test mixture was exposed to the LED light for 20 min. Crosslinking was assessed via a tube inversion test [20] every 30 seconds during light exposure, and the gelation time was recorded for each formulation.

2.7. Animal Model

For *in vivo* studies, a subcutaneous human xenograft tumor model was established in nude mice. Female nude mice (Balb/c nu/nu) with an average body weight of about 20 g were purchased from NCI (Frederick, Maryland). Animals were housed in appropriate isolated caging with sterile rodent food and acidified water *ad libitum* and a 12-h light/dark cycle. A hind leg tumor xenograft was established from a human squamous cell carcinoma (FaDu) tumor cell line. FaDu cells (ATCC, Manassas, VA) were cultured as a monolayer in tissue culture flasks containing minimal essential medium (MEM) supplemented with Earle's salts, L-glutamine, 10% heat-inactivated FBS, 100 U/ml penicillin, 100 μg/ml streptomycin and 0.25 μg/ml amphotericin B (Gibco, Carlsbad, CA). Cultures were grown at 37 °C with 5% CO_2 in air. The right hind leg of each mouse was implanted subcutaneously with 1×10^6 FaDu cells in 30 μl of PBS. Tumors were allowed to grow to around 150 mm^3 before starting treatment, typically 7–9 days after inoculation. Mice were carefully monitored throughout for general well-being, body weight loss, and tumor volume. All animal experiments were performed in accordance with the Duke University Institutional Animal Care and Use Committee.

2.8. *In vivo* NIR Imaging and Fluorophore Retention

Fifteen athymic female nude mice were inoculated with FaDu cells and allowed to grow tumors as previously described. Mice were divided into three groups and received different treatments. The Ce6-cELP+LED group received an intratumoral infusion of a mixture of Ce6-cELP and IRDye800-cELP, followed by 20 min of 660-nm LED exposure (170 mW/cm^2). The Ce6-cELP group was given with the same mixture of Ce6-cELP but did not receive any LED exposure. Finally, the cELP+LED group was infused with a mixture of cELP and IRDye800-cELP (without Ce6) and was then exposed to LED. The mixture of Ce6-cELP and cELP was prepared with a total cELP concentration of 2 mM and a Ce6 concentration of 150 μM. The LED power was consistently maintained at 170 mW/cm^2 for 20 min in all of the mice. The mixture of Ce6-cELP and IRDye800-cELP (0.2 nM IRDye800) was injected intratumorally using a motorized microsyringe pump system (Hamilton, Reno, NV) at a rate of 120 μL/min. In order to observe the interstitial diffusion of cELP during CED infusion, the tumor was imaged using fluorescent molecular tomography (FMT) every 5 μL of the infusion and stopped when the entire tumor area was covered. For ensuring consistent cELP gelation and stability, the LED lamp was held ~2cm away from the tumor site on all mice. Simultaneously, a small handheld fan was placed close to the tumor to prevent skin burning due to overheating. Ce6 control group mice were not given LED exposure. All mice were then imaged using a FMT System 2500 LX (PerkinElmer, Boston, MA) and fluorescent intensity within the tumor was quantified using TrueQuant software (PerkinElmer). Imaging was done 0 h, 24 h, 48 h, 72 h and 168 h after administration of the cELP. Retention at a time point was determined by taking the relative ratio of fluorescent intensity value at the time point to the intensity at 0 h.

2.9. *In vivo* Radionuclide Retention of cELP

Fifteen female nude mice were inoculated and allowed to grow tumors as previously described. Mice were divided into the same three experimental groups as described in Section 2.8, but using ^{125}I-labeled ELP (20 μCi per mouse) instead of fluorophore-labeled ELP. All mice were then measured for ^{125}I radioactivity using an Atomlab 400 Dose Calibrator (Biodex Medical Systems, Shirley, NY). Radioactivity measurements were done 0 h, 24 h, 48 h, 72h and 168 h after administration of the cELP depot. Retention was determined by taking the ratio of ^{125}I radioactivity at each time point to the baseline radioactivity in the mouse at 0 h.

2.10. Biodistribution of [^{125}I]cELP

Mice were intratumorally infused with the same [^{125}I]Ce6-cELP solution as described in section 2.9. At 0, 24, 48 and 72 h after administration, the mouse was dissected and the following organs were harvested: blood, tumor, skin, muscle, thyroid, heart, lungs, liver, spleen, and kidneys. Blood was collected from the orbital socket using glass pipette tips (Denville Scientific, South Plainfield, NJ). Individual organ radioactivity levels were measured using the gamma counter. Biodistribution data were expressed as relative radioactivity in each organ per gram of tissue.

2.11. Tumor Growth Inhibition of PRCITD-Delivered Therapy

FaDu tumors were established in nude mice, as described above. After the tumor size reached 150 mm^3, treatment group mice were intratumorally infused with a formulation of 2 mM cELP and Ce6 at 50, 100, 150 or 200 μM followed by 660-nM LED photoradiation (170 mW/cm^2, 20 min). Control group mice were intratumorally infused with the same dose of cELP and Ce6, but without LED exposure. Each mouse's tumor volume and body weight were monitored daily for the first week, and every other day until the end of the study. Tumor volume was determined using the following equation: volume = $(width)^2 \times length \times \pi/6$. An individual blinded to the identity of the groups took the measurements. Using the same animal tumor model described previously, the antitumor efficacy study of PRCITD-delivered brachytherapy (BT) was conducted with different treatments to investigate the combination therapy effect of BT and PDT co-delivered by this PRCITD. In this study, the animals bearing FaDu tumors were divided into 4 groups: (1) the BT group, whose mice were intratumorally infused with 3 mM [^{131}I]cELP, which undergoes thermal transition at body temperature; (2) the PDT group, whose mice received intratumoral infusion of Ce6-cELP (200μM Ce6, 2 mM cELP) followed by 20 min of LED exposure; (3) the BT+PDT group, whose mice were intratumorally infused with a formulation of Ce6-cELP (200μM Ce6, 2 mM cELP) and 2 mM [^{131}I]cELP and exposed to LED light for 20 min, and (4) the cELP only group, whose mice were infused with unlabeled cELP as a negative control. All mice receiving 131I were dosed with 6.6 μCi/mm^3 tumor, which was a sub-efficacious dose for FaDu tumor treatment as per our previous study [19]. The mice's body weight and tumor volume were monitored as described previously.

2.12. Statistical Methods

Data from the in vitro and in vivo retention studies, as well as all the tumor growth inhibition studies were analyzed with a 1-way ANOVA based on treatment group followed by Scheffe's post-hoc test; $P<0.05$ was considered statistically significant in all cases.

3. Results and Discussion

In this study, we developed a photoradiation-controlled intratumoral depot (PRCITD) system capable of spatiotemporally controlling intratumoral coverage and retention to deliver photodynamic therapy in combination with radionuclide brachytherapy for solid tumors. It was composed of a soluble, naturally occurring polypeptide and was conjugated to the photosensitizer Ce6. Delivery and distribution concerns were overcome using an intratumoral CED injection strategy. Tumor coverage and dose uniformity was evaluated and tracked using fluorescence molecular tomography. Once whole tumor coverage was predicted, extrinsic LED light was to be targeted on the tumor to trigger crosslinking and form a durable hydrogel for sustained anti-cancer therapy, consisting both of photodynamic ROS therapy and radionuclide therapy.

3.1. Characterization of cELP

Ce6 was conjugated to the cELP by N-terminal carboxyl-amine conjugation in the presence of DCC and NHS, as shown in Figure 2A. The reaction efficiency was characterized by measuring 280-nm and 400-nm absorption of the purified product, corresponding to the

respective to cELP and Ce6 concentrations. Concentrations of cELP ranged from 1–3 mM and those of Ce6 ranged from 300–400 μM. Next, the thermal properties of the cELP-Ce6 conjugate were characterized in mouse serum over a range of concentrations in order to ensure solubility at physiological body temperature. The transition temperature (T_t) for cELP-Ce6 was 43.2°C, 40.0°C, and 33.7°C for concentrations of 1 mM, 2 mM, and 3 mM (Figure 2B). As the temperature in the core of subcutaneous tumors in mice is typically ~35 °C (data not shown), cELP-Ce6 concentrations ≤ 2 mM were used in subsequent experiments to prevent thermal transitioning at this temperature.

3.2. Optimization of in vitro gelation conditions

Photoradiation (PR) of the injected Ce6-ELP conjugate at 660-nm may allow for control over the diffusion of the cELP depot prior to its cross-linking compared to the peroxide-based cross-linking that was used previously [20], because the timing of ELP crosslinking is possible to be controlled through scheduling when the tumor is exposed to light for producing $^1O_2$. The latter yield is dependent on the PS concentration and light power [31]. In addition, increasing the number of cysteine residues (cELP concentration) will offer a greater density of cysteine residues for ROS-mediated cross-linking [20, 32], thereby increasing the stability of the depot within the tumor. To determine the optimal conditions, we assessed the effects of cELP concentration, Ce6 concentration, and LED exposure duration on the PRCITD *in vitro* gelation time. As shown in Figure 3A, the speed of cELP gelation was directly proportional to the cELP concentration when Ce6 concentration and LED power were held constant. Additionally, hydrogel formation time exhibited a linear dependence on Ce6 concentration for a cELP concentration of 2000μM and LED power (Figure 3B). However, gelation speed did not increase at Ce6 concentrations above 150 μM (data not shown). Thus, optimal cELP crosslinking could be achieved by preparing a PRCITD mixture of 2 mM cELP loaded with 150 μM Ce6 and exposing it to 660-nm LED light (170 mW/cm^2) for ≥10 min. Figure 3C illustrates that cELP only crosslinks when it is both conjugated to Ce6 and exposed to light (far right). Without either Ce6 or the 660nm photoradiation, the mixture remains completely soluble. The optimal cELP formula and LED power conditions obtained from this study provided a basis for subsequent studies.

In previous work demonstrated by the Chilkoti et al, it has been shown that conjugation of multiple hydrophobic small molecules on the end of a polypeptide can induce micelle self-assembly if the conjugate logD < 1.5. This has been demonstrated in the micelle self-assembly of with CP-DOX [32] and CP-PTX [33] conjugates. While the conjugation of Ce6 was originally considered for potentially driving self-assembly, a singular Ce6 conjugation is insufficient hydrophobicity to provide diblock amphiphilicity to form micelles. By ensuring, loading cELP was only labeled with Ce6 at a 1:1 maximum ratio, the cELP would maintain its soluble, polymeric uniform structure.

3.3. Photodynamic cELP crosslinking improves *in vitro* radionuclide retention

We previously demonstrated that delivering radioiodine inside thermally transitioned ELP can prevent dehalogenation [19]. As radionuclides halogens are easily susceptible to *in vivo* dehalogenation mechanisms, sequestration and protection of the radionuclide structure is important. Specifically, ortho-position of iodine on the hydroxyphenyl group of tyrosine is

readily deiodinated by thyroid hormones [33]. For the PRCITD system, we expected that the sequestration of the [^{125}I]cELP within the gel network would decrease from exposure to deiodinase, improving radionuclide retention. This is critical for tumor radiotherapy, as it is important to have stable iodine on the cELP throughout its radioactive lifespan. The ability of cELP gels to retain ^{125}I was assessed by incubating the crosslinked [^{125}I]cELP gel in fresh mouse plasma at 37°C. At various time points, the serum was removed from the gel, and both components were measured for retained ^{125}I radioactivity. Over 50% of the ^{125}I was retained in the cELP gel even after a week of incubation in mouse serum at 37°C (Figure 4). These results suggest that PRCITD hydrogels could prevent radioiodine dehalogenation and suggested further testing as an *in vivo* drug delivery system.

3.4. Visualization of intratumoral cELP distribution

For interventional drug therapy of deep-seated tumors, such as the liver, prostate and pancreas, MRI, CT, fluorescent microscopy, ultrasound and SPECT are all employed as clinical imaging methods to quantitatively gauge tumor distribution and retention of anticancer agents [34, 35]. For controlling the spatiotemporal distribution of the PRCTID system, we labeled the cELP with a NIRDye800 so that we could continuously image its delivery with FMT as we infused it into our tumor xenografts. Our goal with this approach was to control the whole tumor coverage of the cELP before crosslinking the depot into a stabilized hydrogel. As such, it was critical to determine the time-point when the soluble cELP was fully dispersed throughout the entire tumor interstitium. As Figure 5 shows, FMT imaging showed the corresponding tumor coverage increase due to convection enhanced delivery as the injection volume was incremented. Our drug delivery system has the potential to be developed into a clinically relevant system capable of controlling both tumor retention and coverage.

3.5. Intratumoral cELP crosslinking improved the tumor retention of the payload

Our next objective was two-fold: ensure durable retention of a payload in the tumor through *in situ* gelation while also controlling the soluble polypeptide-drug distribution throughout the tumor interstitium. This was important for ensuring that the PRCITD system could selectively concentrate our anticancer agent, radionuclide therapy, in the tumor and spare the surrounding healthy tissue. Retention of the cELP gel was tracked using time elapsed FMT imaging while radionuclide stability was monitored by administering [^{125}I]-labeled cELP and co-tracking the depots radioactivity.

When compared with controls lacking Ce6 or LED exposure (Figure 6A), the fluorescent intensity of the tumors treated with the full PRCITD system (Ce6-cELP with LED light) was significantly higher than that any of the controls (1-way ANOVA and post hoc test, $P<0.05$) at 4, 24, 48, 72 and 168 hours after administration. FMT visualization of the hydrogels (Figure 6B) confirmed depot retention within the tumor one week after administration. Both controls showed negligible retention confirming the importance of crosslinking for better retention. Next, the tumor retention of ^{125}I in the cELP depot with and without LED exposure were compared (Figure 6C). The results showed that the radioactivity in the tumors treated with Ce6-cELP with LED light exposure was significantly higher than the

radioactivity in the controls at 24, 48, 72 and 168 hours after intratumoral administration (Student *t*-test, $P < 0.05$).

The results also suggest that the radionuclide remains closely associated with the crosslinked cELP for prolonged periods of time, presumably indicating that the *in vivo* photoradiation-triggered cELP gelation reduces the loss of the radionuclide. It is well known that the dehalogenation of peptides and proteins usually occurs via an enzymatic process [36], and protecting the iodine from these enzymes ultimately improves efficacy of radiotherapy. As proteins, dehalogenases are high molecular weight species, and are unlikely to penetrate a crosslinked cELP network. Without access to the interior of the gel network, the gelation of cELP prevents release and subsequent clearance of free iodine. This added benefit of the PRCITD could possibly be conferred to other antitumor agents in future applications. Based on these tumor retention results, we conclude that photoradiation-triggered cELP gelation holds the potential to deliver both photosensitizer and radionuclides for solid tumor treatment with PDT and interstitial brachytherapy.

3.6. Ce6 dose-dependent photodynamic therapy delivered by PRCITD

With the enhanced retention abilities of the PRCITD system confirmed, the photodynamic therapy potential of the depot was next assessed in a growth inhibition study against FaDu tumor xenografts. Formulations of 2 mM cELP were prepared with a range of photosensitizer doses: 50, 100, 150 and 200 μM of Ce6. Each was intratumorally injected into 150 mm^3 tumors and subsequently exposed to 660-nm LED light for 20 minutes. The results (Figure 7) show that significant tumor growth inhibition was achieved through day 5 in a Ce6 dose dependent (1-way ANOVA, $P<0.05$). The lowest dose of 50 μM did not show significant tumor growth inhibition at any time point when compared to the unlabeled ELP group (Scheffe post hoc test, $P<0.05$). The 100 μM and 150 μM groups exhibited significant tumor growth inhibition only through days 3 and 4 (both $P<0.05$). Interestingly, the 200 μM group showed statistically significant inhibition only on Days 3 – 5 compared to the control. This dose-dependent study was a pilot study which only showed a significant difference at three time points (3–5 days) after treatments at a higher concentration range (100 – 200 μM). Ce6 labeling is currently limited to two sites on the cELP. Higher Ce6 concentrations could be explored in the future by recombinantly incorporating additional lysine for increasing the conjugation residues into the cELP sequence. While significant tumor growth delay was achieved at a Ce6 dose of 200 μM, complete regression probably will require a higher concentration of Ce6 for PDT monotherapy.

In future studies, we will also consider the effect of tumor center hypoxia on the efficacy of PDT, which requires oxygen for singlet oxygen production. We hope to maximize tumor regression by combining it with a therapeutic approach that can overcome the resistance due to hypoxia. Many treatments to overcome hypoxia-mediated resistance have been investigated and can be used for this purpose. For example, the efficacy of high dose radiation for hypoxic tumors has been evaluated [37]. Pre-radiation therapy could attain the same effect by reducing interstitial fluid pressure for the re-oxygenation of the hypoxic area [38]. Furthermore, nanoparticles are an attractive platform to overcome drug resistance. PRCITD may provide a new avenue of approach for targeting hypoxic regions by confining

the high radiation dose to the hypoxic area. CED infusion can overcome the limitation of poor tumor penetration, and *in situ* crosslinking can immobilize the depot within the desired area such as the tumor center. This is a setting where we envision a combination therapy with a therapeutic radionuclide such as ^{131}I would yield improvements in a potentially synergistic manner.

3.7. Tumor growth inhibition of combined therapy delivered by the PRCITD

Finally, the tumor growth inhibition in a FaDu tumor models was assessed when the PRCITD system was used to co-deliver the combination therapy of radionuclide brachytherapy and PDT. In previous studies, we have shown that thermally responsive ELPs can deliver ^{131}I to tumors and achieve >67% tumor curing rate in both subcutaneous and orthotopic prostate cancer tumor models at dose of 10 μCi/mm^3 tumor [39]. In order to evaluate potential combination effects, we utilized a sub-lethal dose of 6.6 μCi/mm^3 tumor in this study. As expected, the combination of treatment group (Figure 8) exhibited a significant tumor inhibition advantage (1-way ANOVA, $P<0.05$) from both the cELP-only control and the PDT monotherapy group (Scheffe test, $P<0.05$). Retaining the radioactivity within the tumor by *in situ* gelation provided significant benefit in the therapy of solid tumors. Although this combination trended towards greater effectiveness than either monotherapy, the combination effect was not wholly satisfactory as full tumor regression was unsuccessful. We believe there could be several possible reasons for these results. First, tumor retention of radioiodine delivered by PRCITD was not as high as that delivered by thermally transitioned ELP (56% vs. 82% after 1 week) [39], thus the effective biological dose was much less than the planned dose of 6.6 μCi/mm^3. The longer time required to stabilize the cELP into a hydrogel (20 min after infusion for PRCITD) compared to the near immediate aggregation observed in thermal delivery systems might have contributed to the lower tumor retention. It should be possible to improve tumor retention by increasing the cysteine content in cELP to enhance PRCITD depot stability, which should significantly reduce the time-to-gelation. Increasing the gelation speed further should reduce the loss of the payload during CED infusion. Second, PDT efficacy was Ce6 dose-dependent and 200 μM was the highest concentration we could prepare due to limited free amines on the cELP. Efficacy of the combination therapy might be increased by increasing the Ce6 dose. In future studies, we can increase the number of free amines for Ce6 conjugation by inserting more lysine in the cELP sequence. Third, PDT-based antitumor efficacy is oxygen-dependent and may not be as effective in the hypoxic tumor center as in the normoxic tumor periphery. Therefore, we can expect higher antitumor efficacy if we can concentrate the PDT in the normoxic area. In turn, by minimizing the effects of BT on the surrounding healthy tissue, we can deliver higher doses of radioactivity with BT to central hypoxic regions and attempt to overcome the resistance of hypoxic tumor cells to the therapy. In addition, to address the concern that the photosensitizer (PS) and radionuclide egress from the cELP depot in tumor, leading to excessive PS and radiation exposure of normal tissues, we monitored the body weight of the mice receiving the highest dose of Ce6 at 200 μM and all the groups of the combination study. In addition, the biodistribution of the cELP following photoradiation-triggered gelation was assessed. During the course of PDT, none of the animals exhibited significant clinical signs of toxicity and one of important organs exhibited > 3% of injection dose accumulation (Figure 1 in Supplement Data). This is

encouraging with respect to minimizing off-target side effects of a hydrogel-payload formulation.

4. Conclusion

Our initial study presents an approach to overcome current limitations of *in situ* injectable hydrogel drug delivery systems. Many current technologies maximize tumor coverage at the expense of sacrificing high retention of the payload. Our proposed cELP system proposes to overcome this limitation by the introduction of photodynamic mechanism as a stabilizing element. The flexibility of our cELP system is also beneficial; different types of payloads including radionuclides and chemotherapeutics can be used for maximizing anti-tumor efficacy against different tumor types. This cELP system could be particularly beneficial in a brachytherapy application, where, instead of implanting several metal seeds containing radioactivity as is traditionally done, the cELP with a radioactive payload could be injected once, as a liquid, and form a stable radioactive hydrogel with the aid of external photoradiation.

Supplementary Material

Refer to Web version on PubMed Central for supplementary material.

Acknowledgments

The work was supported by the NIH R01CA138784 and Duke Cancer Institute grants to WL.

References

1. South CP, Khoo VS, Naismith O, Norman A, Dearnaley DP. A comparison of treatment planning techniques used in two randomised UK external beam radiotherapy trials for localised prostate cancer. Clinical oncology. 2008; 20:15–21. [PubMed: 18054471]
2. Gulec SA, Sztejnberg ML, Siegel JA, Jevremovic T, Stabin M. Hepatic structural dosimetry in (90)Y microsphere treatment: a Monte Carlo modeling approach based on lobular microanatomy. Journal of nuclear medicine: official publication, Society of Nuclear Medicine. 2010; 51:301–310.
3. Blair HF, Porter A, Chen QS. In vivo detection of an 125I seed located in the intracardiac region after prostate permanent brachytherapy. Int J Radiat Oncol Biol Phys. 2004; 58:888–891. [PubMed: 14967446]
4. Hrycushko BA, Li S, Goins B, Otto RA, Bao A. Direct intratumoral infusion of liposome encapsulated rhenium radionuclides for cancer therapy: effects of nonuniform intratumoral dose distribution. Med Phys. 2011; 38:1339–1347. [PubMed: 21520844]
5. Kurtz JM, Kinkel K. Breast conservation in the 21st century. Eur J Cancer. 2000; 36:1919–1924. [PubMed: 11000571]
6. Weinberg BD, Blanco E, Gao J. Polymer implants for intratumoral drug delivery and cancer therapy. Journal of pharmaceutical sciences. 2008; 97:1681–1702. [PubMed: 17847077]
7. Willatt JM, Francis IR, Novelli PM, Vellody R, Pandya A, Krishnamurthy VN. Interventional therapies for hepatocellular carcinoma. Cancer imaging: the official publication of the International Cancer Imaging Society. 2012; 12:79–88. [PubMed: 22487698]
8. Dreher MR, Liu W, Michelich CR, Dewhirst MW, Yuan F, Chilkoti A. Tumor vascular permeability, accumulation, and penetration of macromolecular drug carriers. Journal of the National Cancer Institute. 2006; 98:335–344. [PubMed: 16507830]
9. Bobo RH, Laske DW, Akbasak A, Morrison PF, Dedrick RL, Oldfield EH. Convection-enhanced delivery of macromolecules in the brain. P Natl Acad Sci USA. 1994; 91:2076–2080.

10. Lieberman DM, Laske DW, Morrison PF, Bankiewicz KS, Oldfield EH. Convection-enhanced distribution of large molecules in gray matter during interstitial drug infusion. J Neurosurg. 1995; 82:1021–1029. [PubMed: 7539062]
11. Song D, Wientjes MG, Au JL. Bladder tissue pharmacokinetics of intravesical taxol. Cancer chemotherapy and pharmacology. 1997; 40:285–292. [PubMed: 9225946]
12. French JT, Goins B, Saenz M, Li S, Garcia-Rojas X, Phillips WT, Otto RA, Bao A. Interventional therapy of head and neck cancer with lipid nanoparticle-carried rhenium 186 radionuclide. Journal of vascular and interventional radiology: JVIR. 2010; 21:1271–1279. [PubMed: 20478719]
13. Kim Y, Seol DR, Mohapatra S, Sunderland JJ, Schultz MK, Domann FE, Lim TH. Locally targeted delivery of a micron-size radiation therapy source using temperature-sensitive hydrogel. Int J Radiat Oncol Biol Phys. 2014; 88:1142–1147. [PubMed: 24495593]
14. Hruby M, Pouckova P, Zadinova M, Kucka J, Lebeda O. Thermoresponsive polymeric radionuclide delivery system--an injectable brachytherapy. European journal of pharmaceutical sciences: official journal of the European Federation for Pharmaceutical Sciences. 2011; 42:484–488. [PubMed: 21324355]
15. Liu W, Dreher RM, Furgeson DY, Peixoto VK, Yuan H, Zalutsky MR, Chilkoti A. Tumor Accumulation, Degradation and Pharmacokinetics of Elastin-Like Polypeptides in Nude Mice. J Control Release. 2006; 116:170–178. [PubMed: 16919353]
16. Mackay JA, Chilkoti A. Temperature sensitive peptides: engineering hyperthermia-directed therapeutics. International journal of hyperthermia: the official journal of European Society for Hyperthermic Oncology North American Hyperthermia Group. 2008; 24:483–495.
17. Meyer DE, Kong GA, Dewhirst MW, Zalutsky MR, Chilkoti A. Targeting a genetically engineered elastin-like polypeptide to solid tumors by local hyperthermia. Cancer Res. 2001; 61:1548–1554. [PubMed: 11245464]
18. Betre H, Liu W, Zalutsky MR, Chilkoti A, Kraus VB, Setton LA. A thermally responsive biopolymer for intra-articular drug delivery. J Control Release. 2006; 115:175–182. [PubMed: 16959360]
19. Liu W, MacKay JA, Dreher MR, Chen M, McDaniel JR, Simnick AJ, Callahan DJ, Zalutsky MR, Chilkoti A. Injectable intratumoral depot of thermally responsive polypeptide-radionuclide conjugates delays tumor progression in a mouse model. J Control Release. 2010; 144:2–9. [PubMed: 20117157]
20. Asai D, Xu D, Liu W, Garcia Quiroz F, Callahan DJ, Zalutsky MR, Craig SL, Chilkoti A. Protein polymer hydrogels by in situ, rapid and reversible self-gelation. Biomaterials. 2012; 33:5451–5458. [PubMed: 22538198]
21. Dolmans DEJGJ, Fukumura D, Jain RK. Photodynamic therapy for cancer. Nat Rev Cancer. 2003; 3:380–387. [PubMed: 12724736]
22. Dougherty TJ, Marcus SL. Photodynamic therapy. Eur J Cancer. 1992; 28A:1734–1742. [PubMed: 1327020]
23. Jeong H, Huh M, Lee SJ, Koo H, Kwon IC, Jeong SY, Kim K. Photosensitizer-Conjugated Human Serum Albumin Nanoparticles for Effective Photodynamic Therapy. Theranostics. 2011; 1:230–239. [PubMed: 21562630]
24. Li LB, Xie JM, Zhang XN, Chen JZ, Luo YL, Zhang LY, Luo RC. Retrospective study of photodynamic therapy vs photodynamic therapy combined with chemotherapy and chemotherapy alone on advanced esophageal cancer. Photodiagnosis and photodynamic therapy. 2010; 7:139–143. [PubMed: 20728836]
25. Chan HH, Nishioka NS, Mino M, Lauwers GY, Puricelli WP, Collier KN, Brugge WR. EUS-guided photodynamic therapy of the pancreas: a pilot study. Gastrointestinal endoscopy. 2004; 59:95–99. [PubMed: 14722560]
26. Braichotte DR, Wagnieres GA, Bays R, Monnier P, van den Bergh HE. Clinical pharmacokinetic studies of photofrin by fluorescence spectroscopy in the oral cavity, the esophagus, and the bronchi. Cancer. 1995; 75:2768–2778. [PubMed: 7743484]
27. Sibata CH, Colussi VC, Oleinick NL, Kinsella TJ. Photodynamic therapy in oncology. Expert opinion on pharmacotherapy. 2001; 2:917–927. [PubMed: 11585008]

28. Meyer DE, Chilkoti A. Purification of recombinant proteins by fusion with thermally-responsive polypeptides. Nature biotechnology. 1999; 17:1112–1115.
29. Kim JY, Choi WI, Kim M, Tae G. Tumor-targeting nanogel that can function independently for both photodynamic and photothermal therapy and its synergy from the procedure of PDT followed by PTT. J Control Release. 2013; 171:113–121. [PubMed: 23860187]
30. Unak T, Akgun Z, Yildirim Y, Duman Y, Erenel G. Self-radioiodination of iodogen. Appl Radiat Isot. 2001; 54:749–752. [PubMed: 11258523]
31. Lee S, Zhu L, Minhaj AM, Hinds MF, Vu DH, Rosen DI, Davis SJ, Hasan T. Pulsed diode laser-based monitor for singlet molecular oxygen. Journal of biomedical optics. 2008; 13:034010. [PubMed: 18601555]
32. Pragatheeswaran AM, Chen SB. Effect of Chain Length of PEO on the Gelation and Micellization of the Pluronic F127 Copolymer Aqueous System. Langmuir: the ACS journal of surfaces and colloids. 2013; 29:9694–9701. [PubMed: 23855644]
33. Roghani M, Mansukhani A, Dell'Era P, Bellosta P, Basilico C, Rifkin DB, Moscatelli D. Heparin increases the affinity of basic fibroblast growth factor for its receptor but is not required for binding. J Biol Chem. 1994; 269:3976–3984. [PubMed: 8307953]
34. Turner DC, Moshkelani D, Shemesh CS, Luc D, Zhang H. Near-infrared image-guided delivery and controlled release using optimized thermosensitive liposomes. Pharmaceutical research. 2012; 29:2092–2103. [PubMed: 22451250]
35. Zhang Y, Zhang B, Liu F, Luo J, Bai J. In vivo tomographic imaging with fluorescence and MRI using tumor-targeted dual-labeled nanoparticles. International journal of nanomedicine. 2014; 9:33–41. [PubMed: 24368885]
36. Engler D, Burger AG. The deiodination of the iodothyronines and of their derivatives in man. Endocr Rev. 1984; 5:151–184. [PubMed: 6376077]
37. Chao KS, Bosch WR, Mutic S, Lewis JS, Dehdashti F, Mintun MA, Dempsey JF, Perez CA, Purdy JA, Welch MJ. A novel approach to overcome hypoxic tumor resistance: Cu-ATSM-guided intensity-modulated radiation therapy. Int J Radiat Oncol Biol Phys. 2001; 49:1171–1182. [PubMed: 11240261]
38. Multhoff G, Vaupel P. Radiation-induced changes in microcirculation and interstitial fluid pressure affecting the delivery of macromolecules and nanotherapeutics to tumors. Frontiers in oncology. 2012; 2:165. [PubMed: 23162794]
39. Liu W, McDaniel J, Li X, Asai D, Quiroz FG, Schaal J, Park JS, Zalutsky M, Chilkoti A. Brachytherapy using injectable seeds that are self-assembled from genetically encoded polypeptides in situ. Cancer Res. 2012; 72:5956–5965. [PubMed: 23155121]

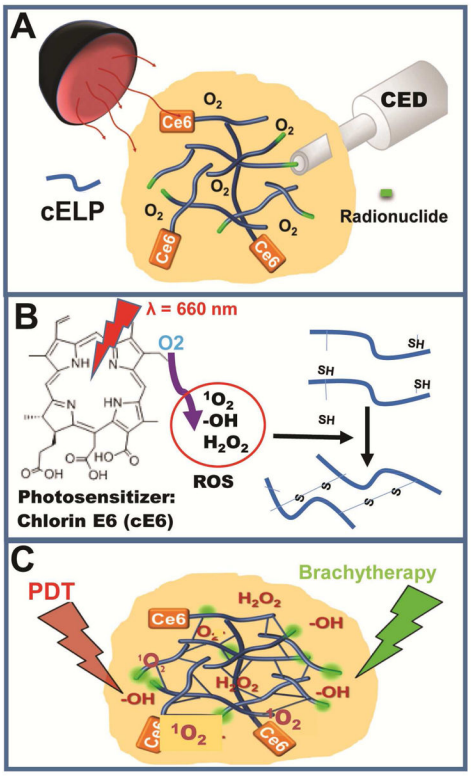

Figure 1.

Schematic illustrating an overview of the approach for development of PRCITD. A) Soluble cELP loaded with photosensitizer and radionuclide freely distribute in tumor driven by CED. B) Photoradiation–generated ROS initiate cELP crosslinking to stabilize the delivery depot; C) PRCITD simultaneously delivers Ce6 and radionuclide for combination therapy.

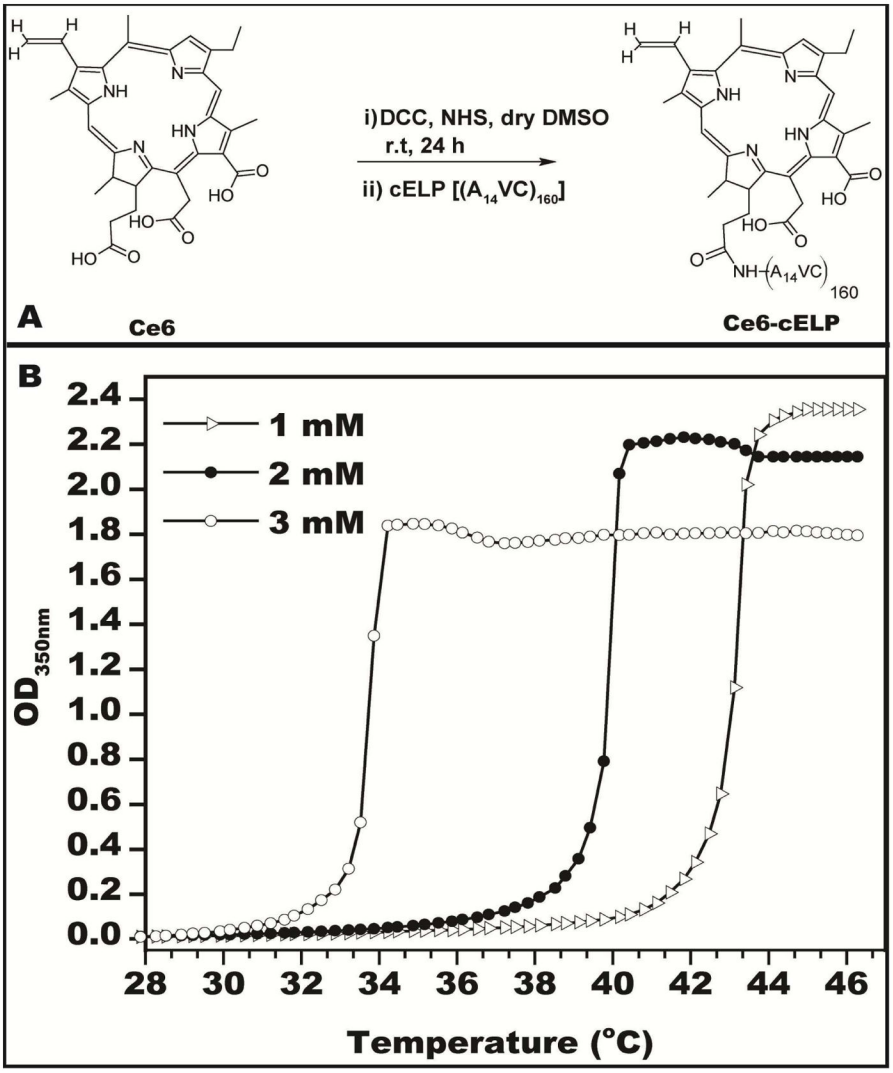

Figure 2.

Characterizations of Ce6-cELP. (A) Reaction scheme for Ce6 conjugation to cELP. (B) Transition temperature measurement of cELP-Ce6 at various concentrations.

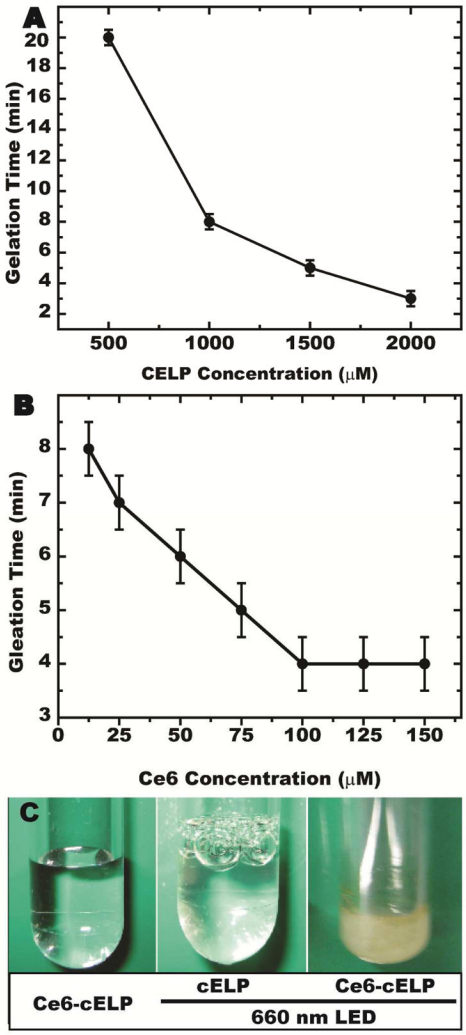

Figure 3.

Photoradiation-triggered *in vitro* cELP crosslinking was examined at different cELP concentrations (A) and different Ce6 concentrations (B). The cELP gel formed at the optimal conditions was imaged (C).

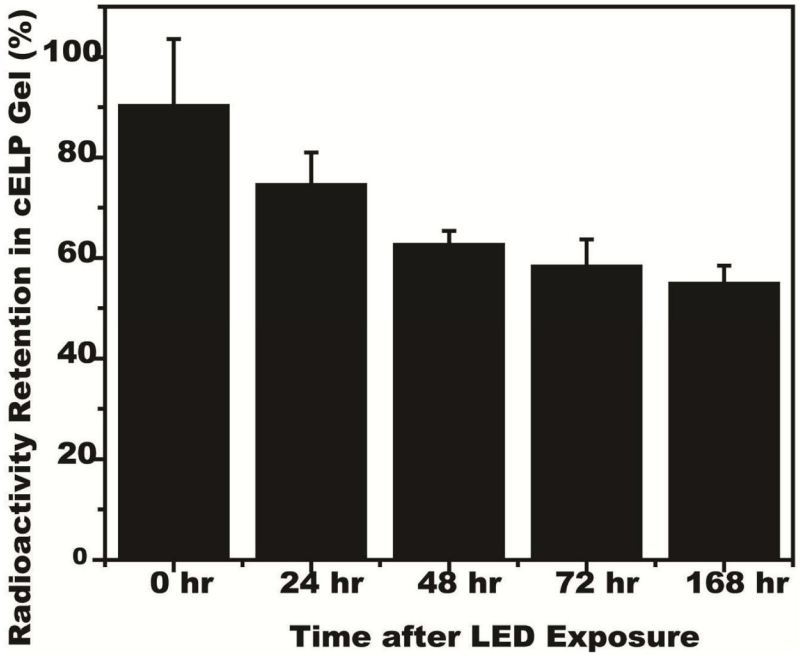

Figure 4.

Radionuclide retention in crosslinked [^{125}I]cELP gel after incubation in mouse serum at 37°C. The percentage of ^{125}I retention at 0, 24, 48, 72 h and 1 week after cELP gelation are expressed as mean (n = 4–5); error bars, SEM.

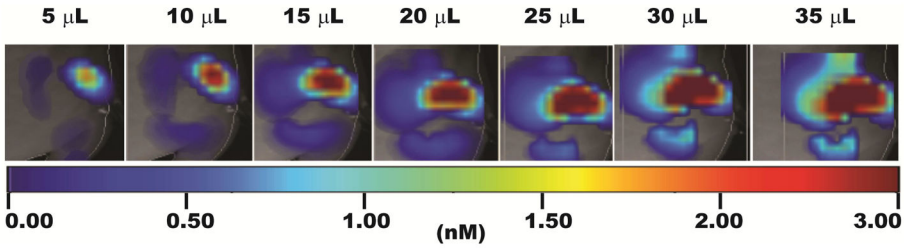

Figure 5.

Fluorescence molecular tomography (FMT) visualization of tumor coverage of soluble injected cELP depot; the injection was carried out as serial intratumoral infusions of 5 μL.

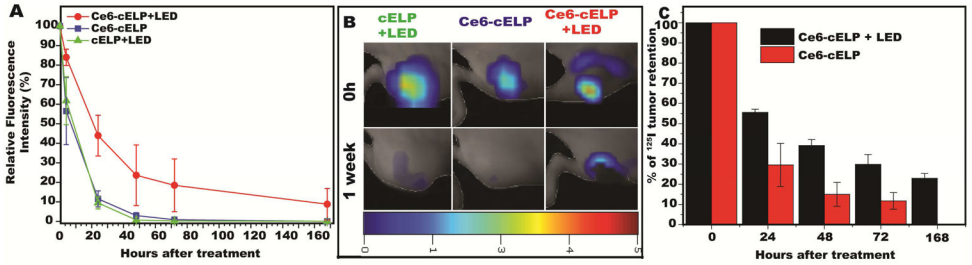

Figure 6.

Intratumoral retention and visualization of cELP depots. All formulations contained 2 mM cELP, and one or both of 150 μM Ce6 and 20 min exposure to 660-nm LED light. (A) Intratumoral retention of fluorophore (IRDye800) over the course of 1 week. Relative fluorescent intensity expressed as mean ± SE, n = 5–6. (B) Fluorescence molecular tomography (FMT) imaging of IRDye800-labeled cELP at time zero and one week. (C) Intratumoral retention of radionuclide (^{125}I) over the course of 1 week, relative radioactivity expressed as mean ± SE, n = 5–6.

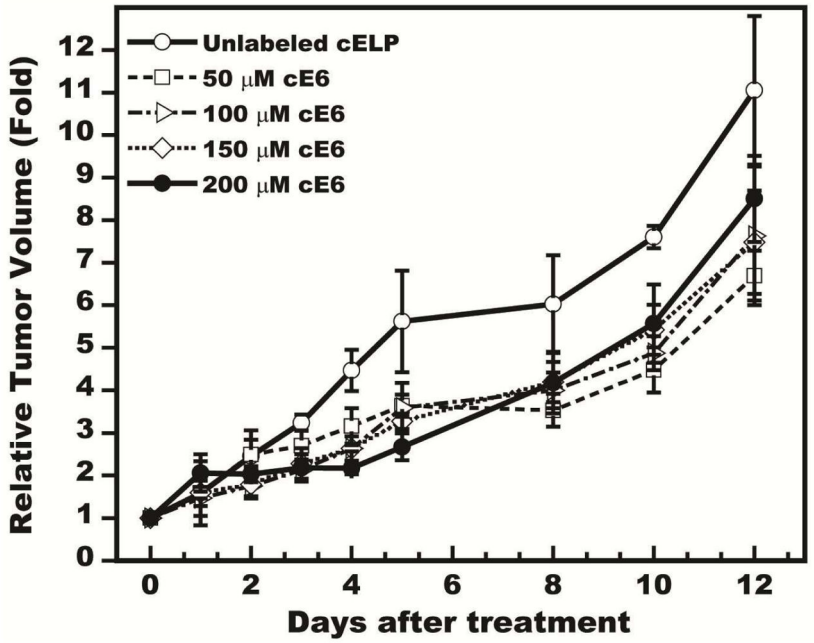

Figure 7.

Dose-dependent tumor growth inhibition of Photosensitizer (Ce6) delivered by PRCITD. Data expressed as relative tumor volume, normalized to initial tumor volume; mean ± SEM, n = 4–5.

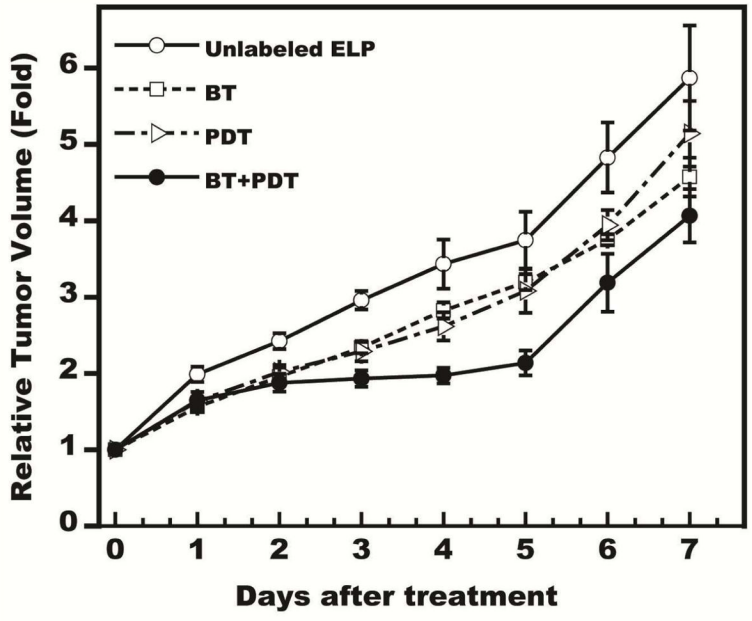

Figure 8.

Tumor growth inhibition of combination therapy (photodynamic and radionuclide) delivered by PRCITD. Data expressed as relative tumor volume, normalized to initial tumor volume; mean ± SEM, n = 5–6.